Oxidation of platinum surfaces and reaction with carbon monoxide

2008 J. Phys.: Condens. Matter 20 184022

(http://iopscience.iop.org/0953-8984/20/18/184022)

IOP Publishing Journal of Physics: Condensed Matter

J. Phys.: Condens. Matter **20** (2008) 184022 (7pp) doi:10.1088/0953-8984/20/18/184022

Oxidation of platinum surfaces and reaction with carbon monoxide

Wei-Xue Li

State Key Laboratory of Catalysis, Dalian Institute of Chemical Physics, Chinese Academy of Sciences, Dalian 116023, People's Republic of China
and
Center for Theoretical and Computational Chemistry, Dalian Institute of Chemical Physics, Chinese Academy of Sciences, Dalian 116023, People's Republic of China

E-mail: wxli@dicp.ac.cn

Received 24 July 2007, in final form 18 September 2007
Published 17 April 2008
Online at stacks.iop.org/JPhysCM/20/184022

Abstract

Identification of structures of active sites of catalysts under realistic conditions is key for understanding the structure–reactivity relationship and mechanism of catalytic reactions. Various *in situ* techniques and novel theoretical concepts (e.g. *ab initio atomistic thermodynamics*) have been developed. As an example, oxidation of stepped Pt(110) and Pt(332) surfaces has been studied using density functional theory, scanning tunneling microscopy and high resolution x-ray photoemission spectroscopy. It was found that ridge Pt atoms are highly reactive and one-dimensional (1D) oxide stripes form along the Pt ridge. Within the 1D oxide stripes, the reactivity is low, and reaction occurs only at the defect sites and/or boundaries of 1D PtO_2 stripes. Furthermore, for stepped Pt(332) surfaces, a site highly active in promoting carbon monoxide (CO) oxidation was identified due to the formation of novel transition states at the boundary of the 1D oxide and chemisorption domains. Since the ratio of the ridge atoms increases with decrease of the particle sizes, the present study highlights the importance of the 1D oxide components for the reactivity of supported nanosize catalysts.

(Some figures in this article are in colour only in the electronic version)

1. Introduction

For decades, surface science study (under ultrahigh vacuum and at low temperatures) of single-crystalline transitional metal surfaces has been driven by the desire to obtain a fundamental understanding of the catalytic reactions on supported catalysts under realistic conditions [1, 2]. Although valuable insights in terms of the adsorption sites, energetics, possible reaction intermediates and even reaction mechanisms have been obtained, it is clear now that for fully uncovering the mechanism of catalytic reactions and bridging the so-called 'materials gap' and 'pressure gap' between surface sciences and realistic catalytic reactions, *in situ* or operand characterization and preparation of realistic model catalysts in a controlled way and synergetic action of advanced theoretical simulations are prerequisite [3–10].

One of the prominent examples related to this is the oxidation reactions, which cover wide ranges of industrially important reactions and environmental protections, for example, selective oxidation, oxidative dehydrogenation, automotive exhaust, corrosion and erosion. Under oxidizing conditions, the catalyst itself may have a tendency to be oxidized, depending sensitively on the temperatures and oxygen partial pressures. Correspondingly, reaction mechanisms change [11]: on metallic surfaces, where a Langmuir–Hinshelwood mechanism is involved, all reactants from the gas phases adsorb on the surfaces, react and desorb from the surfaces. On oxidized surfaces, where the so-called Mar–van Krevlen mechanism is concerned, a distinct feature is that some products of the reaction leave the solid catalyst surfaces with one or more constituents of the catalyst lattice [12]. These have been illustrated clearly by intensive studies (experimentally and theoretically) of oxidation and reactivity of 4d transition metal surfaces (Ru, Rh, Pd and Ag) recently [13–50].

In the present work, the oxidation of 5d transition metal platinum surfaces and its effect on the reactivity, particularly for CO oxidation, are discussed. It is known that for close-packed Pt(111), only an ordered chemisorption phase at a quarter of a monolayer (ML) was observed, and the surfaces

became rough at higher oxygen partial pressures and elevated temperatures [51–53]. Although the high activity of oxidized Pt(110) in promoting CO oxidation has been reported by Frenken and co-workers [4, 5], the microscopic understanding and the mechanism behind remained lacking however, and studies were hence made. For the formation of the oxide, it was presumed that it nucleates at defect sites (for example along the step edge) due to its coordination being unsaturated, and may therefore be crucial for further oxidation. To address this point, the oxidation of vicinal Pt(332) surfaces was studied [54]. Since there are abundant step edges present for the supported catalyst particles, oxidation of the vicinal surfaces under oxidizing conditions and its effects on the activity may be used in a proper model system for real catalytic reactions.

2. Methodologies

Thanks to density functional theory (DFT), dramatic increase of supercomputer power and advanced algorithms allowing us to study complex systems efficiently, first-principles calculations are now used routinely and reliably to obtain detailed information on adsorption structures, energetics, electronic and vibrational properties etc, which are well documented in the literature [55–60]. Furthermore, the reactivity can be evaluated by exploring potential energy surfaces to extract activation barriers and rate constants explicitly. The information obtained can be compared quantitatively with experiments. For the study of oxide formation of transition metal surfaces, which will be discussed in detail here, it is noted that the determination of structures formed under oxidizing conditions, a prerequisite for further reactivity study, still represents a significant challenge from both experimental and theoretical points of view due to the lower symmetry and uncertain stoichiometry. In most cases, a combination of theory and element specific, structure sensitive and *in situ* techniques, such as high resolution x-ray photoemission spectroscopy (XPS) [61], atomic resolution STM [62] and *in situ* surface x-ray diffraction (SXRD) [63], to name just a few, is essential, as illustrated clearly in the following.

Although chemical bond breaking and making as well as detailed structures can be well described using DFT, the effects of environmental factors, such as temperature (T) and partial pressure (p), which are crucial to the formation and stability of various structures, are still lacking because of the nature of the ground state (absolute zero). It is therefore very important to incorporate T/p in the theoretical simulations, which have been developed recently using so-called *ab initio atomistic thermodynamics* [24, 64, 65]. Using this methodology, various structure models with different coverage and periodicity can be compared directly, and a phase diagram for a wide range of T/p can be constructed from density functional theory calculations. From this phase diagram, the formation of the thermodynamically most favorable structures can be identified. In reality, the formation of the thermodynamically most stable structures may however be kinetically hindered. Correspondingly, a metastable structure may present as the active phase, and the reactivity and reaction mechanism may be modified, accordingly. Nevertheless, the novel methodology provides a starting point for studying catalytic reaction under given realistic reaction conditions. The detailed principles/applications of *ab initio* atomistic thermodynamics as well as its correlation with kinetics can be found in excellent review articles from the literature [66, 67].

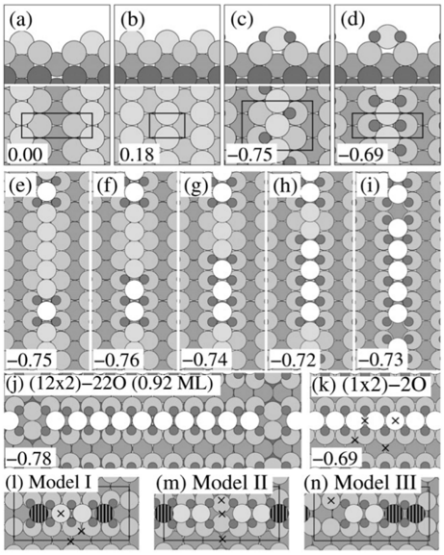

Figure 1. ((a), (b)) Clean Pt(110) structures: the numbers refer to the formation energies (in eV) of the surface per (1 × 2) unit area with respect to the reconstructed surface. (a) The reconstructed and (b) unreconstructed Pt(110) surface. ((c)–(n)) Oxidized Pt(110) structures: the formation energies (in eV) per O are given. (c) Pt(110)-(2 × 2)-2O (0.5 ML). (d) Pt(110)-(1 × 2)-2O (1.0 ML). (e) Pt(110)-(6 × 2)-4O (0.33 ML). (f) Pt(110)-(6 × 2)-6O (0.50 ML). (g) Pt(110)-(6 × 2)-8O (0.67 ML). (h) Pt(110)-(6 × 2)-10O (0.83 ML). (i) Pt(110)-(6 × 2)-12O (1.00 ML, one ridge Pt atom ejected). (j) Pt(110)-(12 × 2)-22O (0.92 ML, two ridge Pt atoms ejected). (k) Same as (d). ((l)–(n)) Pt(110)-(6 × 2) models I–III of part of the structure in (j). The crosses indicate the CO adsorption sites. (From [69].)

3. Oxidation of Pt(110)

Oxygen chemisorption and oxidation on the Pt(110) surface have been extensively studied theoretically and experimentally. Whether the thin surface oxides play a role under realistic conditions is still a subject to be investigated. So far, Frenken and co-workers [4, 5] have shown that Pt(110) must reconstruct into one of several possible surface oxide structures to yield high $O_2 + CO$ reaction rates. The detailed interaction between oxygen and Pt(110) from lower to higher oxygen loading as well as its reactivity as regards CO oxidation however remain unknown and are discussed in the following.

3.1. Chemisorption and oxidation

For clean Pt(110) surfaces, the reconstructed missing row (1 × 2) surface (figures 1(a) and (b)) is a ground state structure, forming a (111) facet on the side of the edge to lower the surface energy [68, 69]. For modest oxygen exposures up to 10 L at room temperature, STM measurements found bright

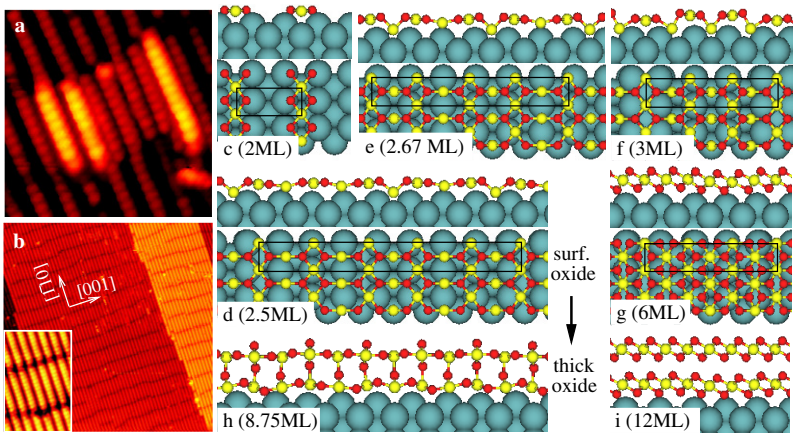

Figure 2. STM images of the Pt(110) surface after exposure to (a) 60 min atomic O at 500 K. High resolution image (60×60 Å^2) of a surface oxide island. (b) 75 min atomic O at 600 K (500×500 Å^2). Insets: high resolution image (46×77 Å^2) of the (12×2)-2O chemisorption and/or surface oxide phase. Ball-and-stick models of (c) the chemisorption, ((d)–(g)) surface oxide, and ((h), (i)) thicker oxide structures modeled with DFT. Red, yellow, and blue spheres (small black, small grey and large spheres in the printed version of the journal): oxygen, oxidic, and metallic platinum atoms. Please note that the definition of the 2 ML in this figure is equivalent to 1 ML plotted in figure 2 (from [7]).

stripes on the Pt ridges, which were assigned to PtO_2 units involving ridge Pt atoms and a local 1.0 ML of O bound in fcc sites on the (111) nanofacets of the ridges [70, 71]. At a stripe coverage above 0.04 ML, stripes on adjacent Pt ridges tend to align along the [001] direction, perpendicular to the Pt ridges, namely, the configuration consists of O covered ridges of finite length rather than an extended phase that minimizes the energetic cost of terminating the stripes [72]. According to DFT calculations, the structure of the extended phase with the highest O binding energy consists of a 1.0 ML structure of fully O covered ridges ((1×2)-2O (1 ML)), as shown in figure 1(d) with oxygen chemisorption energy -0.69 eV per O. Such structures are not allowed to relax in the $[1\bar{1}0]$ direction. Using DFT, we found considerable surface stresses, 0.295 eV Å^{-2} and -0.150 eV Å^{-2} in the $[1\bar{1}0]$ direction for the clean and 1.0 ML O covered ridges, respectively. Since the stresses have opposite signs, the realization of a mixed structure of alternating clean and O covered regions will allow stress relief of both regions. This was indeed found by experimental measurements and theoretical calculations, where Pt ridge atoms within stripes are expanded by 4% compared to the bare ridge, and the overall energy gain due to this relaxation with respect to the 1.0 ML O structure is 74 meV per O. In figures 1(e)–(h), models with stripes of PtO_2 units with different lengths in supercells of an arbitrary fixed length, namely six Pt nearest-neighbor distances in the $[1\bar{1}0]$ direction, are shown. The total oxygen coverage increases from 0.33 to 0.83 ML. The adsorption potential energies per oxygen decrease slightly (numerically) from -0.75 eV at 0.33 ML to -0.72 eV at 0.83 ML oxygen, due to the increase of repulsion within the stripes.

The repulsion can however be released by ejecting certain Pt ridge atoms, as found by experiments, figures 2(a) and (b), by exposure of the surface to atomic oxygen at 500 and 600 K [7], and modeled in figures 1(i) and (j), where one and two Pt atoms have been removed for every six ((6×2)-12O (1 ML)) and twelve Pt atoms ((12×2)-22O (0.92 ML)), and the Pt–Pt distance within the stripes is calculated to increase by 7% and 8.1%, respectively. The stress relief compensates the energy cost of formation of Pt vacancies, and the overall formation energies are -0.73 eV/O and -0.78 eV/O, which result in energy gains of 0.04 and 0.09 eV per O over 1 ML structure. The latter structure is not a simple chemisorption structures, since it involves ejecting of the Pt atoms and significant structure distortion, and we refer to these below as surface oxide models. Similar structure has been observed and characterized on Rh(110) [34, 35]. Three-dimensional oxide islands have been observed at 500 K (figure 2(a)). On the basis of this, growth of bulk oxide α-PtO_2 has been developed and is shown schematically in figures 2(c)–(i).

On the basis of the oxygen chemisorption structures and surface oxide models in figure 1, we have constructed the surface free energy diagram and plotted it in figure 3, for Pt(110) in the presence of an O_2 gas. The thermodynamic parameters of the O_2 gas are described by the chemical potential, $0.5 \times \Delta\mu_{O_2}$ (noted as $\Delta\mu_O$ in figure 3 and below). The O_2 partial pressures corresponding to $\Delta\mu_O$ at a temperature of 300 K are shown in the figure. The shaded background in the diagram marks the range of $\Delta\mu_O$ where bulk α-PtO_2 is thermodynamically favored ($\Delta\mu_O > 0.5 \times \Delta H(PtO_2) = -0.82$ per PtO_2 unit). In agreement with STM experiments [7] we found the Pt(110)-(12×2)-22O surface oxide to be energetically favorable for a large range of $\Delta\mu_O$. The calculated thicker oxides (not shown in figure 3) are less favorable than surface oxide. The existence of the three-dimensional oxide island found by experiments may come from the kinetics hindrance and stabilization due to the presence of the defects.

3.2. Reactivity

The reactivity of the oxidized Pt(110) and a-PtO_2 with respect to CO oxidation have been studied by searching for the minimum potential energy path (MEP) taking us from CO(g)

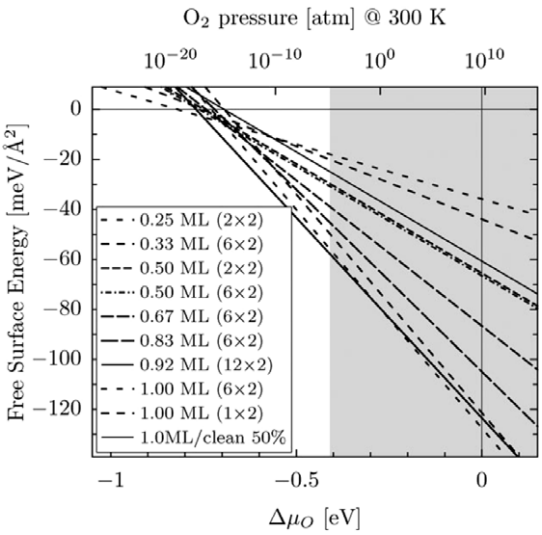

Figure 3. Free surface energy diagram. The reference is the clean (1 × 2) reconstructed Pt(110) surface depicted in figure 1(a). The legends refer in order of appearance to the structures: (1) 0.25 ML O in bridge sites along the Pt ridge; (2) figure 1(e); (3) figure 1(c); (4) figure 1(f); (5) figure 1(g); (6) figure 1(h); (7) figure 1(j); (8) figure 1(i); (9) figures 1(d) and (k); (10) a reconstructed surface covered to 50% by large islands of the 1 ML structure, figure 1(d). The shaded area identifies the region where bulk a-PtO_2 is thermodynamically preferred. (From [69].)

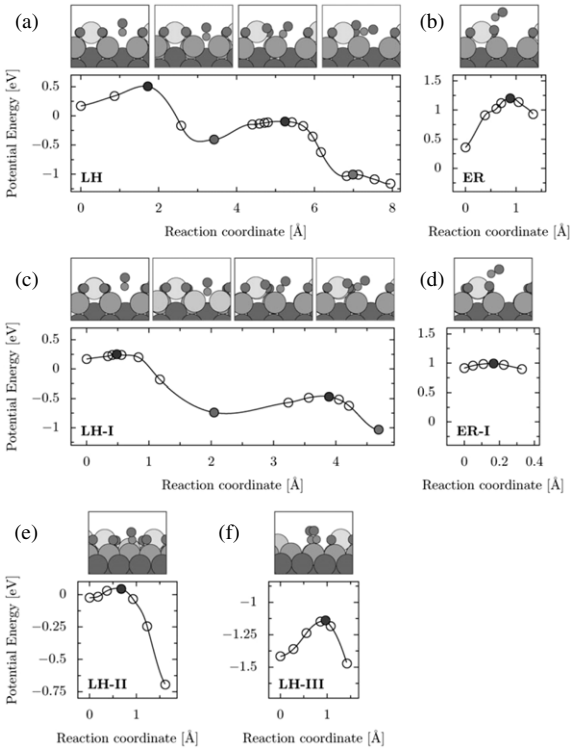

Figure 4. CO oxidation on models of the surface oxide covered Pt(110). The energy zero is for CO far from the surfaces. (a) CO adsorption and subsequent oxidation via an LH type of reaction on Pt(110)-(1 × 2)-2O modeled in a (2 × 2) cell. (b) Oxidation via an ER mechanism on the same surface. ((c)–(f)) CO oxidation on Pt(110)-(12 × 2)-22O using models I–III. (c) Model I: CO adsorption and subsequent oxidation via an LH type of reaction. (d) Model I: oxidation via the ER mechanism. (e) Model II: the LH type of oxidation of CO between two stripes. (f) Model III: LH oxidation of CO adsorbed at the boundary of the CO saturated (1 × 1) surface and the (12 × 2) oxide surface. (From [69].)

and the oxidized surface to CO_2(g) and the surface with a vacancy. The CO oxidation step can happen either through the Eley–Rideal (ER) mechanism in which the CO reacts directly from the gas phase with an oxygen atom from the surface or via the Langmuir–Hinshelwood (LH) mechanism in which the CO adsorbs, diffuses and finally reacts with an adsorbed oxygen atom.

The CO oxidation on Pt(110)-(1×2)-2O structure in (2×2) cells, which is used to model the surface oxide, lacks the stress relief present in the true surface oxide. The structure is plotted in figure 1(k), where crosses indicate the CO adsorption sites. In figures 4(a) and (b) we display the potential energy with respect to CO in the gas phase at certain points along the LH and ER reaction pathways on the Pt(110)-(1 × 2) surface. For the LH reaction, we find an adsorption barrier of 0.5 eV, and the most stable adsorption site is the long bridge site in the trough, and the adsorption energy is −0.41 eV calculated using the revised Perdew–Burke–Ernzerhof functional (RPBE) [59]. In the transition state towards CO_2 formation, the CO is adsorbed in an atop site of the inclined (111) nanofacet of the ridge and the nearest O is pushed upwards and slightly away from the CO. The calculated CO oxidation barrier is only 0.3 eV which is more than 0.4 eV smaller than for the reaction on Pt(111) [73, 74]. For the ER reaction we calculate a much higher CO oxidation barrier than in the LH case.

The CO oxidation on the surface oxide (12 × 2)-22O is too large to simulate. To make the calculations feasible, we built some smaller (6 × 2) models of part of the surface oxide I–III, which are shown in figures 1(l)–(n). Models I and II are meant for studying the middle and terminal parts of the PtO_2 stripes in the continuous (12 × 2) reconstruction, while model III was built to enable the modeling of the reactivity at the phase boundary between the (12 × 2) reconstructed island and a bare (or CO covered) metallic part of the Pt(110) surface. For CO oxidation on model I, CO 'prefers' to adsorb on the same site as Pt(110)-(1×2)-2O as discussed above, but with stronger bonding by 0.30 eV (the adsorption energy −0.74 eV (RPBE)) due to the expansion of the PtO_2. The calculated potential energy profile (figure 4(c)) is almost identical to that of the LH energy diagram of the (1 × 2) structure, figure 4(a). Since the reference energy of CO in the gas phase is unaffected by whether the PtO_2 stripe is expanded or not, the overall reaction barrier is lowered by 0.3 eV approximately. CO adsorption at the boundary between stripes (model II, figure 4(e)) is almost neutral, and the calculated barrier for CO oxidation is 0.1 eV, which seems to be an active channel. The three-phase boundary structure of model III (figure 4(f)) turns out to be quite reactive. The CO adsorption energy at the atop site is −1.41 eV (RPBE), and the oxidation barrier of the CO reacting with an oxygen atom from the end of the PtO_2 stripe is only 0.3 eV, correspondingly.

For CO oxidation on bulk α-PtO_2, it turns out to be unlikely, either due to the large CO adsorption barrier (1.9 eV)

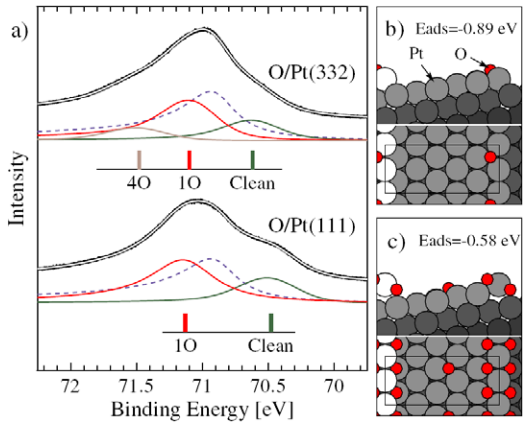

Figure 5. (a) Pt $4f_{7/2}$ core-level spectra for O/Pt(332) and O/Pt(111) after saturation with oxygen at 310 K. In the decompositions, the dashed blue line is for the bulk. ((b), (c)) Calculated equilibrium structures and average adsorption potential energy at (b) low and (c) high O coverage. (From [54].)

on the perfect pristine (0001) surface, or the diffusion barrier on the surface with oxygen vacancy. The $(10\bar{1}0)$ facet is however found to be ready for CO adsorption and following oxidation, with an overall barrier less than 0.3 eV. These studies show a small reaction barrier for the CO oxidation on the Pt(110)-(12×2)-22O surface oxide and on the open α-PtO_2 $(10\bar{1}0)$ surfaces, which are in qualitative agreement with the experiments by Frenken and co-workers [4, 5].

4. Oxidation of the vicinal Pt(332) surface

The adsorption of, and reactions amongst, molecules are often very different at steps than on the flat parts of the particle surfaces, which may therefore profoundly influence the catalytic properties of the surfaces [75–77]. The altered adsorption and reaction behavior is often ascribed to the fact that the lower coordination number at a step modifies the electronic structure in its vicinity and that the molecules may adsorb in new geometrical configurations at steps [78]. In addition to these effects, the steps may also be significantly modified by one or more of the reactant molecules through local compound formation occurring as an integral part of the reaction. Such compound formation may be expected to occur more easily at steps because of the larger freedom for geometrical rearrangements there than on flat parts of the surface. The possibility of compound formation is of particular relevance in oxidation reactions, since typical catalyst materials all have a high propensity for oxide formation, which will be discussed below.

The oxidation of the stepped Pt(332) surface, which is composed of (111) terraces six atomic rows wide and a (111) type step, was studied by means of DFT calculations and XPS measurements [54]. In figure 5, we show Pt $4f_{7/2}$ core spectra obtained after saturation of the Pt(332) and Pt(111) with O as achieved by a $p \approx 10^{-6}$ Torr O_2 exposure for 500 s at 310 K. Both spectra contain a bulk component (dashed line) at 70.90 eV, a component at 70.5 eV ('clean') from surface Pt atoms not coordinating to any O, and a component at 71.1 eV ('1O') from Pt atoms coordinating to one chemisorbed O. The spectrum for O/Pt(332) further contains a high energy component ('4O') not present in the spectrum for O/Pt(111). The saturated coverage is 0.25 monolayers on Pt(111) (ML; 1 ML equals the number of Pt atoms in one (111) layer) and 0.42^{111}ML on Pt(332) (where the designation ^{111}ML refers to the density of Pt in the (111) surface).

On the basis of the amount of oxygen and measured O 1s and Pt $4f_{7/2}$ spectra, DFT calculations lead us to propose this O structure on Pt(332), which is depicted in figure 5(c). The structure has an O coverage of $0.46\ ^{111}$ML, with four out of five oxygen atoms bonding to the step Pt. Every step Pt is fourfold coordinated to O (hence the designation 4O above), and the step can thus be described as a repeated 1D PtO_2 unit, an oxide stripe. For Pt 4f (figure 5(a)), using a clean terrace of Pt as the reference, we calculate shifts of -0.51 and -0.81 eV for the terrace Pt bonding to one O, and the Pt within the PtO_2 stripe. These numbers are in excellent agreement with the measured values of -0.5 ± 0.07 and -0.85 ± 0.07 eV for 1O and 4O, respectively. The structure in figure 5(c) is also consistent with the experimental finding of a significant intensity for the clean component in figure 5(a). The high coverage structure (figure 5(c)) is preferred for oxygen chemical potentials, μ_O, in the range -0.50 eV $< \mu_O < -0.41$ eV, where the lower bound corresponds to the switch to the low coverage structure (figure 5(b)) and the upper bound to the onset of bulk oxide formation. At 310 K the μ_O range translates to the oxygen pressure range, 5×10^{-10} Torr $< p_{O_2} < 8 \times 10^{-2}$ Torr. Given the computational (several orders of magnitude for pressures) and experimental ($\sim$10% for absolute coverages) uncertainties, we identified the high oxygen coverage ($0.46\ ^{111}$ML) structure in this pressure range as being consistent with the experimental findings.

1D PtO_2 oxide is found to be stable on other vicinal Pt(111) surfaces over chemisorption phases at oxygen chemical potentials down to -0.5 eV, which is below the threshold for bulk PtO_2 formation, $\mu_O = -0.41$ eV. Thus, the 1D oxide may serve as a precursor for bulk oxide growth on Pt surfaces, which contain steps and kinks. Considering Pt nanoparticles in catalysis, their steps and edges must hence be expected to undergo 1D oxidation above $\mu_O \sim -0.5$ eV. At 300, 400, and 500 K this corresponds to pressures of $p_{O_2} > 7 \times 10^{-9}$, 6×10^{-4} and 1 bar. Under operating conditions, such nanoparticles may therefore appear as enchained in a 1D oxide network.

The reactivity of these oxide stripes is higher than that of oxygen pre-covered Pt(111) surface, as seen in CO oxidation [54]. Experimental study shows that CO oxidation becomes negligible when the temperature is lower than 220 K. For oxygen pre-covered Pt(111)-(2×2) surfaces, to quench the CO oxidation, the temperature only needs to be lower than 270 K. For temperatures where CO oxidation occurs on both surfaces it has been found that, for the same O pre-coverage on both surfaces, more atomic O is removed from Pt(332) than from Pt(111).

Preferential oxygen removal from the oxide stripes is further supported by DFT calculations. A CO molecule

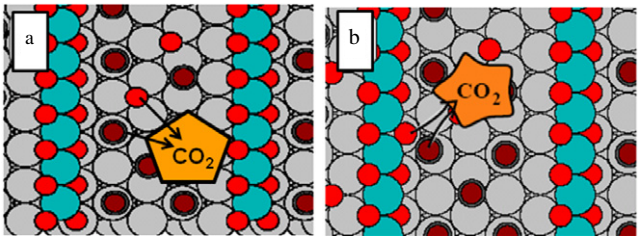

Figure 6. Transition states for CO oxidation with terrace O (a) and bottom O in the PtO_2 stripe (b) on Pt(332) surface.

bonding to the terrace at the foot of the PtO_2 covered step encounters a 0.60 eV energy barrier for forming CO_2 with an oxygen atom extracted from the bottom O row in the PtO_2 stripe. For CO reacting with an oxygen atom in a local $p(2 \times 2)$-$(O + CO)$ structure on the terrace of Pt(332) the barrier is higher, 0.71 eV. The lower barrier must originate from a more favorable transition state being possible at the step, since we do not see the O bond strength in the oxide as the reason for the lower barrier: extracting a single O atom from the PtO_2 covered step costs 0.77 eV [79], whereas removing a single terrace bonded O costs only 0.54 eV. Detailed geometrical analysis of the transition state (TS), as schematically plotted in figure 6, shows that CO approaches the bottom O row in the PtO_2 stripe from a Pt top site via a Pt–Pt bridge site. While CO approaches the terrace O, the CO goes from a Pt top site over a Pt hcp site towards the terrace O, which is required to be activated further from the hollow site to the bridge site. The latter activation is absent for the bottom O row in the PtO_2. This means that it is mainly the availability of the new, favorable TS that causes high reactivity of the 1D PtO_2 oxides.

5. Conclusions

The oxidation of the Pt(110) and Pt(332) surfaces, together with their reactivity as regards CO oxidation, has been discussed in the present work. The high reactivity of step edges due to the lower coordination number leads to the formation of 1D oxide, under conditions where formation of bulk oxide is thermodynamically not favorable yet. Furthermore, the 1D oxide is highly reactive, as evidenced by the CO oxidation, due to the formation of the favorable transition states at the phase boundary. Since the population of the ridge atoms increases with decrease of the size of the particles, the 1D oxide formed under oxidizing conditions may have important implications for the reactivity of the supported catalysts.

Acknowledgments

The author thanks B Hammer, F Besenbacher, J Andersen, E K Vestergaard, S Helveg, M Scheffler, and K Reuter for fruitful discussions and collaborations. The National Natural Science Foundation of China, Chinese Academy of Sciences Bairen Project and Max Planck Society are acknowledged for financial support.

References

[1] Duke C B and Plummer E W (ed) 2001 Frontiers in surface and interface science *Surf. Sci.* **500** 1 (special issue)
[2] Ertl G, Knözinger H and Weitkamp J 1997 *Handbook of Heterogeneous Catalysis* (New York: Wiley)
[3] Over H, Kim Y D, Seitsonen A P, Wendt S, Lundgren E, Schmid M, Varga P, Morgante A and Ertl G 2000 *Science* **287** 1474
[4] Hendriksen B L M and Frenken J W M 2002 *Phys. Rev. Lett.* **89** 046101
[5] Ackermann M D *et al* 2005 *Phys. Rev. Lett.* **95** 255505
[6] Lundgren E M *et al* 2004 *Phys. Rev. Lett.* **92** 046101
[7] Li W X, Österlund L, Vestergaard E K, Vang R T, Matthiesen J, Pedersen T M, Lægsgaard E, Hammer B and Besenbacher F 2004 *Phys. Rev. Lett.* **93** 146104
[8] Ketteler G, Ogletree D F, Bluhm H, Liu H J, Hebenstreit E L D and Salmeron M 2005 *J. Am. Chem. Soc.* **127** 18269
[9] Kresse G, Lundgren E, Bergermayer W, Podloucky R, Koller R, Schmid M and Varga P 2003 *Appl. Phys.* A **76** 701
[10] Lundgren E, Mikkelsen A, Andersen J N, Kresse G, Schmid M and Varga P 2006 *J. Phys.: Condens. Matter* **18** R481
[11] Todorova M, Li W X, Ganduglia-Pirovano M V, Stampfl C, Reuter K and Scheffler M 2002 *Phys. Rev. Lett.* **89** 096103
[12] Doornkamp C and Ponec V 2000 *J. Mol. Catal.* A **162** 19
[13] Over H, Seitsonen A P, Lundgren E, Schmid M and Varga P 2001 *J. Am. Chem. Soc.* **123** 11807
[14] Stampfl C and Scheffler M 1996 *Phys. Rev.* B **54** 2868
[15] Reuter K, Ganduglia-Pirovano M V, Stampfl C and Scheffler M 2002 *Phys. Rev.* B **65** 165403
[16] Reuter K and Scheffler M 2003 *Phys. Rev. Lett.* **90** 046103
[17] Reuter K, Frenkel D and Scheffler M 2004 *Phys. Rev. Lett.* **93** 116105
[18] Rovida G, Pratesi F, Maglietta M and Ferroni E 1974 *Surf. Sci.* **43** 230
[19] Campbell C T 1985 *Surf. Sci.* **157** 43
[20] Carlisle C I, King D A, Bocquet M-L, Cerda J and Sautet P 2000 *Phys. Rev. Lett.* **84** 3899
[21] Li W X, Stampfl C and Scheffler M 2002 *Phys. Rev.* B **65** 075407
[22] Li W X, Stampfl C and Scheffler M 2003 *Phys. Rev.* B **67** 045408
[23] Li W X, Stampfl C and Scheffler M 2003 *Phys. Rev.* B **68** 165412
[24] Li W X, Stampfl C and Scheffler M 2003 *Phys. Rev. Lett.* **90** 256102
[25] Michaelides A, Reuter K and Scheffler M 2005 *J. Vac. Sci. Technol.* A **23** 1487
[26] Schmid M *et al* 2006 *Phys. Rev. Lett.* **96** 146102
[27] Schnadt J, Michaelides A, Knudsen J, Vang R T, Reuter K, Lægsgaard E, Scheffler M and Besenbacher F 2006 *Phys. Rev. Lett.* **96** 146101
[28] Köhler L, Kresse G, Lundgren E, Schmid M, Gustafson J, Mikkelsen A, Borg M, Yuhara J, Andersen J N and Varga P 2004 *Phys. Rev. Lett.* **93** 266103
[29] Gustafson J, Mikkelsen A, Borg M, Lundgren E, Köhler L, Kresse G, Schmid M, Varga P, Torrelles X, Quirós C and Andersen J N 2004 *Phys. Rev. Lett.* **92** 126102
[30] Conrad H, Ertl G, Küppers J and Latta E E 1977 *Surf. Sci.* **65** 245
[31] Zheng G and Altman E I 2000 *Surf. Sci.* **462** 151
[32] Lundgren E, Kresse G, Klein C, Borg M, Andersen J N, De Santis M, Gauthier Y, Konvicka C, Schmid M and Varga P 2002 *Phys. Rev. Lett.* **88** 246103
[33] Gabasch H, Unterberger W, Hayek K, Klötzer B, Kresse G, Klein C, Schmid M and Varga P 2006 *Surf. Sci.* **600** 617
[34] Vesselli E, Africh C, Baraldi A, Comelli G, Esch F and Rosei R 2001 *J. Chem. Phys.* **114** 4221

[35] Africh C, Esch F, Li W X, Corso M, Hammer B, Rosei R and Comelli G 2004 *Phys. Rev. Lett.* **93** 126104
[36] Dudin P, Barinov A, Gregoratti L, Kiskinova M, Esch F, Dri C, Africh C and Comelli G 2005 *J. Phys. Chem.* B **109** 13649
[37] Dri C, Africh C, Esch F, Comelli G, Dubay O, Köhler L, Mittendofer F, Kresse G, Dudin P and Kiskinova M 2006 *J. Chem. Phys.* **125** 094701
[38] Baraldi A, Dhanak V R, Comelli G, Prince K C and Rosei R 1997 *Phys. Rev.* B **56** 10511
[39] Baraldi A, Cerda J, Martyn-Gago J A, Comelli G, Lizzit S, Paolucci G and Rosei R 1999 *Phys. Rev. Lett.* **82** 4874
[40] Norris A G, Schedin F, Thornton G, Dhanak V R, Turner T S and McGrath R 2000 *Phys. Rev.* B **62** 2113
[41] Gustafson J *et al* 2005 *Phys. Rev.* B **71** 115442
[42] Gustafson J *et al* 2006 *Phys. Rev.* B **74** 035401
[43] Bondzie V A, Kleban P and Dwyer D J 1996 *Surf. Sci.* **347** 319
[44] Zheng G and Altman E I 2002 *Surf. Sci.* **504** 253
[45] Saidy M, Warren O L, Thiel P A and Mitchell K A R 2001 *Surf. Sci.* **494** L799
[46] Todorova M, Lundgren E, Blum V, Mikkelsen A, Gray S, Gustafson J, Borg M, Rogal J, Reuter K, Andersen J N and Scheffler M 2003 *Surf. Sci.* **541** 101
[47] Rogal J, Reuter K and Scheffler M 2007 *Phys. Rev. Lett.* **98** 046101
[48] Rocca M *et al* 2000 *Phys. Rev.* B **61** 213
[49] Gajdoš M, Eichler A and Hafner J 2003 *Surf. Sci.* **531** 272
[50] Costina I, Schmid M, Schiechl H, Gajdoš M, Stierle A, Kumaragurubaran S, Hafner J, Dosch H and Varga P 2006 *Surf. Sci.* **600** 617
[51] Saliba N A, Tsai Y L, Panja C and Koel B E 1999 *Surf. Sci.* **419** 79
[52] Parkinson C R, Walker M and McConville C F 2003 *Surf. Sci.* **545** 19
[53] Shumbera R B, Kan H H and Weaver J F 2006 *Surf. Sci.* **600** 2928
[54] Wang J G *et al* 2005 *Phys. Rev. Lett.* **95** 256102
[55] Hohenberg P and Kohn W 1964 *Phys. Rev.* B **136** 864
[56] Kohn W and Sham L 1965 *Phys. Rev.* A **140** 1133
[57] Payne M C, Teter M P, Allan D C, Arias T A and Joannopoulos J D 1992 *Rev. Mod. Phys.* **64** 1045
[58] Perdew I P, Chevary J A, Vosko S H, Jackson K A, Pederson M R, Singh D J and Fiolhais C 1992 *Phys. Rev.* B **46** 6671
[59] Hammer B, Hansen L B and Nørskov J K 1999 *Phys. Rev.* B **59** 7413
[60] Henkelman G and Jonsson H 1999 *J. Chem. Phys.* **111** 7010
[61] Comelli G, Dhanak V R, Kiskinova M, Prince K C and Rosei R 1998 *Surf. Sci. Rep.* **32** 165
[62] Besenbacher F and Nørskov J K 1993 *Prog. Surf. Sci.* **44** 5
[63] Stierle A, Steinhäuser A, Rühm A, Renner F U, Weigel R, Kasper N and Dosch H 2004 *Rev. Sci. Instrum.* **75** 5302
[64] Reuter K and Scheffler M 2002 *Phys. Rev.* B **65** 035406
[65] Łodzianan Z and Nørskov J K 2003 *J. Chem. Phys.* **118** 11179
[66] Reuter K 2006 *Nanocatalysis* ed U Heiz and U Landman (Berlin: Springer) p 343
[67] Reuter K, Stampfl C and Scheffler M 2005 *Handbook of Materials Modeling* vol 1, ed Y Sidney (Berlin: Springer) p 149
[68] Baud S, Ramseyer C, Bihlmayer G, Blugel S, Barreteau C, Desjonqueres M C, Spanjaard D and Bernstein N 2004 *Phys. Rev.* B **70** 235423
[69] Pedersen T M, Li W X and Hammer B 2006 *Phys. Chem. Chem. Phys.* **8** 1566
[70] Helveg S, Lorensen H T, Horch S, Lægsgaard E, Stensgaard I, Jacobsen K W, Nørskov J K and Besenbacher F 1999 *Surf. Sci.* **430** L533
[71] Walker A V and King D A 1998 *J. Chem. Phys.* **109** 6879
[72] Helveg S, Li W X, Bartelt N C, Horch S, Laegsgaard E, Hammer B and Besenbacher F 2007 *Phys. Rev. Lett.* **98** 115501
[73] Alavi A, Hu P, Deutsch T, Silvestrelli P L and Hutter J 1998 *Phys. Rev. Lett.* **80** 3650
[74] Eichler A and Hafner J 1999 *Phys. Rev.* B **59** 5960
[75] Zambelli T, Wintterlin J, Trost J and Ertl G 1996 *Science* **273** 1688
[76] Dahl S, Logadottir A, Egeberg R C, Larsen J H, Chorkendorff I, Törnqvist E and Nørskov J K 1999 *Phys. Rev. Lett.* **83** 1814
[77] Gambardella P, Sljivancanin Z, Hammer B, Blanc M, Kuhnke K and Kern K 2001 *Phys. Rev. Lett.* **87** 056103
[78] Hammer B, Nielsen O H and Nørskov J K 1997 *Catal. Lett.* **46** 31
[79] Li W X and Hammer B 2005 *Chem. Phys. Lett.* **409** 1